Density functional theory and simulation of the columnar phase of a system of parallel hard ellipsoids with attractive interactions

Elvira Martín del Río,* Amparo Galindo, and Enrique de Miguel[†]

Department of Chemical Engineering, Imperial College London, South Kensington Campus, London SW7 2AZ, United Kingdom

A simple molecular model consisting of parallel hard oblate ellipsoids with superimposed square-well attractive interactions of variable range is considered for the study of the phase behavior of thermotropic discotic molecules. A density functional theory appropriate for nonuniform fluids is formulated in which the hard-core contributions to the free energy are treated within a nonlocal weighted-density approximation (WDA) while the attractive contributions are treated at a mean-field level. It is shown that the columnar phase becomes stable relative to the nematic phase at fluid densities for a range of values of the range of the attractive well. In these cases, the region of stability of the columnar phase is bounded at high temperatures by a nematic-columnar-solid triple point. The calculations show that if the attractions are made too long ranged ($\lambda/D \gtrsim 0.84$ for particles of aspect ratio of $L/D=0.1$, where λ/D is the range of the attractive interaction in units of the molecular diameter D), columnar ordering becomes unstable and the nematic phase dominates at all fluid densities. It is shown that columnar ordering is also predicted when the density functional theory is supplemented with the smoothed-density approximation (SDA). Computer simulations have also been carried out for a particular choice of model parameters; our simulation data confirm the stabilization of the hexagonal columnar phase between the solid and nematic phases. A comparison with simulation data allows us to conclude that the WDA provides a fairly good description of the columnar phase and very good agreement for the nematic-columnar transition properties. On the other hand, our calculations show that the SDA largely underestimates the transition pressure and predicts a too-strongly first-order nematic-columnar transition.

I. INTRODUCTION

The ability of highly anisotropic molecules to form liquid-crystal phases, which possess intermediate order between the fully disordered isotropic liquid and the fully ordered crystalline solid, is well established [1–3]. Early works concentrated on elongated molecules, and it is, by comparison, only recently that the existence of liquid crystalline phases of disklike molecules has been confirmed [4,5], and numerous disklike mesogens have now been identified [1,3,6], including suspensions of hard-colloidal platelets [7–10]. The phase behavior of discotic mesogens typically includes nematic (positionally disordered) and columnar (positionally ordered in two dimensions) phases. In the columnar phase the particles are stacked in columns arranged in a two-dimensional lattice, while the particles within a column have liquidlike positional disorder. A number of variants of the columnar phase have been proposed in terms of the space groups of the planar arrangement of the columns, their tilt, and the correlations between the particles within a column (most typically the columns are fluid) or between columns [3]. Understanding the mechanisms that lead to the organi-

zation of oblate (disklike) particles into columnar phases is of current fundamental and practical interest, as these phases can show electronic conductivity along the column's axis for specifically tailored molecules [11]. Furthermore, disklike particles are also of interest in models of clay suspensions [12–14] and in biological fluids [15–17].

Computer simulation studies of hard-body models have been able to confirm the ideas put forward by Onsager [18] that liquid-crystalline phase transitions could be understood in terms of anisotropic excluded-volume interactions and have shown that it is possible to stabilize nematic, smectic, and columnar phases in fluids of both oblate and prolate hard molecules [19–25]. In addition, these simulations have established the importance of the molecular shape in stabilizing the different types of liquid-crystal phases. For example, although hard spherocylinders and hard cut spheres exhibit nematic, and smectic or columnar, liquid-crystalline phases, hard (prolate and oblate) ellipsoids exhibit only a nematic phase [22]. The absence of columnar or smectic phases in such systems has been rationalized in terms of the anisotropic scaling that maps a system of parallel hard ellipsoids into a fluid of hard spheres [25,26]. This excludes the possibility of observing fluid phases with partial translational order in such systems. Similarly, no columnar phase was reported in the early simulations of infinitely thin platelets [19,20], although more recent studies [27,28] point to the existence of the columnar phase in systems of hard cylinders in the limit $L/D \to 0$ (L is the thickness of the cylinder and D its diameter). The onset of columnar ordering has been reported in fluids of hard-cut-sphere platelets of varying aspect ratios [29,30]; a cubic phase was also predicted by the

---

*Permanent address: Departamento de Ingeniería Eléctrica y Térmica, Escuela Politécnica Superior de La Rábida, Universidad de Huelva, 21819 Huelva, Spain.

[†]Author to whom correspondence should be addressed. Permanent address: Departamento de Física Aplicada, Facultad de Ciencias Experimentales, Universidad de Huelva, 21071 Huelva, Spain. Electronic address: demiguel@uhu.es

simulations [29], but this phase has so far not been seen experimentally. By contrast, simulations of perfectly parallel hard cut spheres of aspect ratio $L/D=0.1$ suggest that layered structures characteristic of smectic phases are stabilized in place of columnar phases [31]. Though the study reported in Ref. [31] was limited to a single value of the molecular aspect ratio, it seems to indicate that a degree of orientational freedom is needed to destabilize the solid phase with respect to the columnar phase in models of hard particles.

In spite of the importance of hard-body models, one should bear in mind that interactions in most real systems are not purely repulsive and, in formulating simple models of complex fluids, attractive interactions should also be taken into account; they are responsible for stabilizing phases otherwise not present in hard fluids and provide the temperature-dependent phase behavior crucial for modeling real mesogens. A typical example is provided by the Gay-Berne potential [32]. This model potential incorporates anisotropic attractive interactions to favor side-by-side or face-to-face configurations in systems of prolate or oblate molecules, respectively. It has been very successful in modeling the phase behavior of thermotropic liquid crystals and, for carefully chosen parametrizations, rodlike Gay-Berne particles are seen to exhibit not only nematic phases, but also a variety of smectic phases [33–37]. Parametrizations of the Gay-Berne interactions have also been proposed to model disklike mesogens [38–41], and phase diagrams including columnar phases have been reported. Caprion *et al.* [41] have carried out a systematic study of the effect of the energy anisotropy parameter κ' (the ratio of the edge-to-edge and face-to-face attractive interaction) in this model and find that large anisotropies are required to stabilize the columnar phase. Their study serves as an excellent example of the importance of both the repulsive and attractive contributions to our understanding of the phase behavior of real mesogens. They also highlight an important aspect often neglected in experimental works—the effect of pressure—and construct pressure-temperature phase diagrams for different values of κ'.

Theoretical approaches for systems of nonspherical molecules are far from trivial, especially for the case of phases displaying positional ordering in addition to long-range orientational order (e.g., smectic and columnar phases). A number of studies have been carried out to account for the smectic phase, mostly related to the case of systems consisting of prolate molecules (see Ref. [3] and references therein), but comparatively few have been concerned with columnar ordering in systems of disk-shaped molecules. One reason can be ascribed to the mathematical difficulties associated to the description of anisotropic systems characterized by a strongly varying periodic density wave in two dimensions. An additional difficulty is related to the fact that the Onsager approach, which relies on truncation of the free energy at the level of the second virial coefficient, is justified for long rodlike molecules but is not as accurate for platelets [18].

Early molecular theories for the nematic-columnar transition (see, for instance, Ref. [6]) were formulated as extensions of the McMillan-Kobayashi mean-field theory of the smectic-*A* phase [42,43]. Unfortunately the McMillan-Kobayashi model neglects the excluded-volume interactions

arising from the repulsive interactions at short distances (see Ref. [3] for more details). A more successful formalism to treat positionally ordered phases is provided by a density functional scheme, where the free energy of the system is written as a functional of the one-particle density $\rho(\mathbf{r})$ with the appropriate symmetry [44]. Thus, positional order can be described by allowing $\rho(\mathbf{r})$ to develop modulations along the director (for the smectic phase) or in the transverse plane (for the columnar phase). The density functional formalism has been applied to the study of columnar ordering in systems such as parallel hard spherocylinders [45], parallel hard cylinders [46], and in mixtures of aligned cylinders [47]. In a more recent application, Coussaert and Baus [48] have reported a theoretical study of the columnar phase in systems of discotic Gay-Berne molecules using a density functional theory. The contribution of the repulsive interactions to the excess free energy is treated within the smoothed-density approximation (SDA) [46], and the attractive contributions are incorporated in a perturbative way by making use of a van der Waals–like mean-field approximation. They consider isotropic, nematic, and columnar phases and investigate the phase behavior for various parametrizations of the Gay-Berne potential. Their results are in qualitative agreement with simulation data, although they find that the theory underestimates the stability of the nematic phase; in addition, the isotropic-nematic and nematic-columnar transitions are found to be too strongly first order. Finally, an accurate description of the thermodynamic and structural properties of a dense columnar fluid of hard disks has also been provided by Wensink [49] using a modified cell theory. The resulting expressions are very simple and find excellent agreement with simulation data for both the equation of state and the intercolumnar and intracolumnar spacings. Unfortunately only a hard system has yet been considered.

Here we will be concerned with the description of the columnar phase, highlighting the importance of the coupling between anisotropic short-range repulsions and the longer-ranged attractive interactions in stabilizing columnar ordering in a particularly simple model of disk-shaped molecules. This is of direct relevance to the recent work by Bushby and co-workers [11,50,51] who have been concerned with improving the properties of columnar liquid-crystal materials stabilizing the phases by complementary quadrupolar and van der Waals (dispersion) interactions. They have been able to design materials with higher intracolumnar and intercolumnar order than conventional columnars. It is interesting also to mention the work of van der Kooij *et al.* [52] who have shown the rich phase behavior that can be observed in suspensions of sterically stabilized platelets by inducing attractive depletion interactions mediated through nonadsorbing polymers. In our model, the repulsive and attractive interactions are highly correlated, and even if the attractive interactions have spherical symmetry, the anisotropy of the repulsions are expected to build correlations onto the attractive interactions. This mechanism, which is at the heart of the generalized van der Waals theory for nematics introduced by Gelbart and Baron [53], has been invoked to explain the stability of the smectic phase in model systems of rodlike molecules in a recent work [54]. We follow this idea and investigate whether this mechanism can also stabilize the

two-dimensional ordered columnar phase in a model system of disklike molecules with ellipsoidal symmetry. The model can be considered as a generalized version of the square-well model appropriate for nonspherical molecules and includes both repulsive and attractive interactions, as does the Gay-Berne model, but at a much simpler level. For this purpose, we present a density functional theory based on the weighted-density approximation (WDA) of Tarazona [55] to account for the spatial inhomogeneities of the columnar phase and incorporate the isotropic attractive contributions to the free energy at a mean-field level. At this point we treat the simplest case of parallel molecules. In addition to simplifying the theoretical treatment, this model is of interest since in the case of related models (hard cut spheres) computer simulations indicate that the smectic rather than the columnar phase is stable [31]. We show here that a model of parallel hard oblate ellipsiodal particles with isotropic attractive interactions can give rise to a stable columnar phase and confirm this result by comparison with computer simulation data obtained as part of this work. A comparison of the theoretical predictions with simulation data shows that the WDA provides a far better description of the columnar phase than the simpler SDA.

We describe the generalized anisotropic molecular square-well model in Sec. II. The density functional theory is formulated in Sec. III where we also give details pertaining to the WDA and SDA used here. The theoretical predictions for appropriate values of the molecular parameters are presented and discussed in Sec. IV, together with simulation data and a comparison with the theoretical predictions. Our conclusions are summarized in Sec. V.

II. MOLECULAR MODEL

We consider a fluid system of axially symmetric oblate particles. Orientational fluctuations are disallowed by constraining the symmetry axis of the molecules to remain parallel to a common direction, here taken as the z axis. Thus, the interaction energy contains no explicit dependence on the orientational degrees of freedom. For a pair of molecules located at positions $\mathbf{r}_1$ and $\mathbf{r}_2$, the interaction energy is expressed as

$$u(\mathbf{r}_{12}) = u_{\text{rep}}(\mathbf{r}_{12}) + u_{\text{att}}(\mathbf{r}_{12}), \tag{1}$$

where u_{rep} and u_{att} represent the repulsive and attractive parts of the pair interaction, respectively, and $\mathbf{r}_{12} = \mathbf{r}_2 - \mathbf{r}_1$ is the intermolecular vector. The molecules are assumed to consist of a hard core with ellipsoidal shape determined by its short (L) and long (D) principal axes, the molecular volume being $v_0 = (\pi/6)LD^2$ (see Fig. 1). A measure of the molecular anisotropy is given by the aspect ratio $\kappa = L/D$, with $\kappa < 1$ for oblate molecules. The repulsive pair interaction is therefore given by

$$u_{\text{rep}}(\mathbf{r}_{12}) = \begin{cases} \infty & \text{if } r_{12} \leq \sigma(\hat{\mathbf{r}}_{12}), \\ 0 & \text{if } r_{12} > \sigma(\hat{\mathbf{r}}_{12}), \end{cases} \tag{2}$$

where $\sigma(\hat{\mathbf{r}}_{12})$ is the distance of closest approach between two parallel hard ellipsoids (PHE's). Here, r_{12} is the distance be-
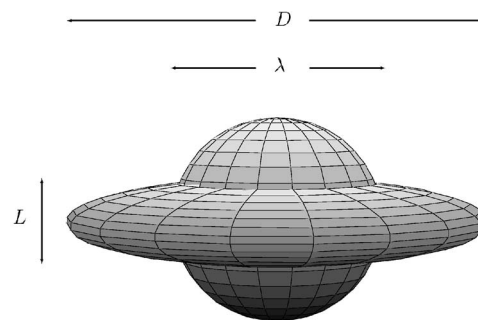

FIG. 1. Generalized square-well model. Molecules consist of a hard oblate core with ellipsoidal symmetry. L is the molecular length along the symmetry axis, and D is the diameter. For oblate molecules $L < D$. The attractive interaction is represented by a square well of range λ. According to the geometry of the model, $\lambda = L$ would correspond to a purely hard ellipsoidal molecule. In this work, we limit ourselves to values of the range parameter $L < \lambda < D$—i.e., $\kappa < \lambda/D < 1$, where $\kappa = L/D$ is the aspect ratio.

tween the molecular centers of mass and $\hat{\mathbf{r}}_{12} = \mathbf{r}_{12}/r_{12}$ is a unit vector along the intermolecular vector. The attractions are modeled by a square-well interaction

$$u_{\text{att}}(\mathbf{r}_{12}) = \begin{cases} -\epsilon & \text{if } \sigma(\hat{\mathbf{r}}_{12}) < r_{12} < \lambda, \\ 0 & \text{if } r_{12} \geq \lambda, \end{cases} \tag{3}$$

where λ is the range and ϵ the strength of the attractive interaction. According to Eq. (3), the attractive pair interaction outside the hard core is spherically symmetric and contains no explicit anisotropic terms.

The model defined by Eqs. (1)–(3) can be regarded as a generalization of the square-well model for simple fluids ($\kappa = 1$) to molecular fluids ($\kappa \neq 1$). Evans *et al.* [56] introduced a similar model consisting of an arbitrary hard nonspherical core embedded in a spherical square well. This choice, however, may lead to a gross overestimation of the range of the attractive interactions for highly nonspherical molecular cores. The model of Evans *et al.*, with the explicit consideration of orientational degrees of freedom, has been applied to the study of nematic liquid crystals with the hard core taken to be either an ellipsoid or a spherocylinder [57–61]. In a more recent study [54], the generalized square-well model defined in Eqs. (1)–(3) has been considered to study the stability of the smectic phase in fluids of prolate molecules with $L/D = 5$, restricting the range of the attractive interactions to values $D < \lambda < L$. As reported in Ref. [54] the model exhibits smectic behavior at fluid densities for a range of values $1.3D \lesssim \lambda \lesssim 4.1D$. Interestingly, for longer attractive ranges smectic ordering is destabilized and the nematic phase dominates the fluid region of the phase diagram.

In this work, we consider parallel oblate molecules defined by an aspect ratio $L/D = 0.1$ and different values of the range of the attractive interactions $L < \lambda < D$. This is expected to be a fair (albeit very simplified) representation of the attractive interactions arising from the aromatic central section of discotic molecules. We should stress that if the attractive interactions were fully neglected ($\lambda = L$), the present model would reduce, under an anisotropic scaling, to

a system of hard spheres. Obviously, columnar ordering is not expected in such limit. The question of whether columnar or crystalline structures are promoted when the attractions are explicitly included is far from trivial and is the subject of this work.

III. DENSITY FUNCTIONAL THEORY

Let us consider a system of disklike molecules in a volume V at a temperature T interacting through the pair potential defined in the previous section. The thermodynamic properties and phase behavior of the system can be analyzed in terms of the Helmholtz free energy. As we are primarily concerned with columnar ordering, we adopt a density functional approach for nonuniform fluids, in which the equilibrium one-particle distribution function $\rho(\mathbf{r})$ is obtained by minimizing the free-energy functional $F[\rho]$. Considering the form of the intermolecular interactions given in Eq. (1), the free energy can be divided into two parts: $F[\rho] = F_{\text{rep}}[\rho] + F_{\text{att}}[\rho]$. F_{rep} is the contribution to the free energy arising from the repulsive interactions. For the molecular model under consideration, this term will correspond to the free energy of a system of parallel hard (oblate) ellipsoids. On the other hand, F_{att} stands for the contribution to the free energy arising from the attractive interactions. The repulsive part can be expressed in terms of the ideal gas contribution and a configurational part:

$$F_{\text{rep}}[\rho] = k_B T \int d\mathbf{r}\, \rho(\mathbf{r})\{\ln[\Lambda^3 \rho(\mathbf{r})] - 1\} + \Delta F_{\text{PHE}}[\rho], \quad (4)$$

where k_B is Boltzmann's constant, Λ is the thermal de Broglie wavelength, and ΔF_{PHE} is the configurational part of the free energy of a system of PHE's. This excess contribution is not known, so that further approximations must be made. A simple local density approximation is not expected to be appropriate to describe the highly oscillatory density profiles that characterize the columnar phase. Following the underlying ideas of the nonlocal density approach set by Tarazona [62], we consider that $\Delta F_{\text{PHE}}[\rho]$ for the inhomogeneous fluid can be approximated by the excess free energy of an equivalent uniform fluid evaluated locally at a coarse-grained density $\bar{\rho}(\mathbf{r})$—i.e.,

$$\Delta F_{\text{PHE}}[\rho] = \int d\mathbf{r}\, \rho(\mathbf{r}) \Delta \psi_{\text{PHE}}(\bar{\rho}(\mathbf{r})), \quad (5)$$

where $\Delta \psi_{\text{PHE}}$ is the excess free energy per particle of a homogeneous system of PHE molecules. The coarse-grained density $\bar{\rho}(\mathbf{r})$ incorporates information about local variations in $\rho(\mathbf{r})$ and is at each point a nonlocal functional of the one-particle distribution function $\rho(\mathbf{r})$. There is no unique way to define $\bar{\rho}(\mathbf{r})$ in terms of the physical density $\rho(\mathbf{r})$. Tarazona [55] has considered the following definition for a nonuniform system of hard spheres (HS's):

$$\bar{\rho}_{\text{HS}}(\mathbf{r}) = \int d\mathbf{r}'\, \rho_{\text{HS}}(\mathbf{r}')w(|\mathbf{r}' - \mathbf{r}|; \bar{\rho}_{\text{HS}}), \quad (6)$$

where $w(r; \rho)$ is a normalized weighting function. Within the WDA, it is assumed that the weighting function can be ex-

pressed as a quadratic expansion in powers of the density:

$$w(r; \rho) = w_0(r) + w_1(r)\rho + w_2(r)\rho^2. \quad (7)$$

Explicit expressions of the w_i functions can be found elsewhere (see, for instance, Refs. [63] and [64]). An alternative definition of the coarse-grained density $\bar{\rho}$ was earlier proposed by Tarazona [62] using a zeroth-order approximation for the weighting function—i.e., $w(r) = w_0(r)$. This is usually referred to as the smoothed-density approximation. Within the SDA, $w(r)$ does not depend explicitly on the density and the calculation of $\bar{\rho}$ from Eq. (6) is straightforward. The calculation of $\bar{\rho}$ through Eqs. (6) and (7) within the WDA is more demanding. Nonetheless, the WDA is expected to provide a better description of dense systems in which the particle density varies strongly [55].

In order to proceed, one should note that a system of PHE's can be transformed into a system of HS's by a simple anisotropic scaling of the Cartesian coordinates. Using this transformation, the distribution functions for the PHE system can be simply obtained from the corresponding distribution functions of a system of hard spheres. Using this transformation, the definition of $\bar{\rho}$ for HS's given in Eq. (6) can be easily generalized to define a coarse-grained density for the PHE system [54,63] as

$$\bar{\rho}(\mathbf{r}) = \int d\mathbf{r}'\, \rho(\mathbf{r} + \mathbf{S}^{-1}\mathbf{r}')w(|\mathbf{r}'|; \kappa \bar{\rho}(\mathbf{r})), \quad (8)$$

where $\mathbf{S}$ is the (diagonal) tensor with components $(1, 1, (\kappa)^{-1})$ that defines the coordinate transformation. An additional consequence of this mapping is that the free energy of the PHE system is simply given by that of a HS system at the same packing fraction. Using the quasiexact Carnahan-Starling expression gives

$$\Delta \psi_{\text{PHE}}(\eta) = k_B T \frac{4\eta - 3\eta^2}{(1 - \eta)^2}, \quad (9)$$

where $\eta = \rho_0 v_0$ is the packing fraction and ρ_0 the average number density.

Finally, the attractive contribution to the free energy is treated at a mean-field level and is given by

$$F_{\text{att}}[\rho] = \frac{1}{2} \int d\mathbf{r}\, d\mathbf{r}'\, \rho(\mathbf{r})\rho(\mathbf{r}')u_{\text{att}}(|\mathbf{r} - \mathbf{r}'|). \quad (10)$$

For a system of parallel molecules, such as the one considered here, the simplest fluid phase corresponds to the nematic phase. In this case, there is no translational order: the phase is spatially uniform and the one-particle distribution function reduces to the average number density—i.e., $\rho(\mathbf{r}) \equiv \rho_0$. In addition, $\bar{\rho}(\mathbf{r}) = \rho_0$. The free-energy functional of the nematic phase becomes a function of the number density (and the temperature) and is explicitly given by

$$\frac{F_N}{V} = f_N = k_B T \rho_0 [\ln(\Lambda^3 \rho_0) - 1] + \rho_0 \Delta \psi_{\text{PHE}}(\rho_0) + \frac{1}{2} \rho_0^2 h_{att},$$

$$(11)$$

where

$$h_{att} = -\frac{4\pi}{3}\epsilon\left[\lambda^3 - \kappa D^3 + \kappa\frac{(D^2 - \lambda^2)^{3/2}}{(1 - \kappa^2)^{1/2}}\right]. \quad (12)$$

In this work we are primarily concerned with the stability of columnar ordering. Recall that the z axis is taken along the common direction of alignment of the molecular axes. The density within the columns is assumed to be uniform, and therefore $\rho = \rho(\mathbf{R})$ with $\mathbf{R} = (x, y)$. After integration along z in Eq. (10) the attractive contribution to the free energy (per unit volume) f_{att} can be written as

$$f_{att} = \frac{1}{2A}\int_A d\mathbf{R}\,\rho(\mathbf{R})h(\mathbf{R}), \quad (13)$$

where A is the section of the system in the x-y plane. We have defined

$$h(\mathbf{R}) = \int d\mathbf{R}'\,\rho(\mathbf{R}')\bar{u}_{att}(|\mathbf{R} - \mathbf{R}'|), \quad (14)$$

with

$$\bar{u}_{att}(R) = \int_{-\infty}^{\infty} dz\,u_{att}(\sqrt{R^2 + z^2}) \quad (15)$$

and $R^2 = x^2 + y^2$. Using the expression for u_{att} given in Eq. (3) and performing the integration in Eq. (15) one obtains

$$\bar{u}_{att}(R) = \begin{cases} -2\epsilon[z_{max}(R) - z_{min}(R)] & \text{if } R < R_{max}, \\ 0 & \text{if } R > R_{max}, \end{cases} \quad (16)$$

where

$$z_{min}^2(R) = \kappa^2(D^2 - R^2), \quad z_{max}^2(R) = \lambda^2 - R^2, \quad (17)$$

$$R_{max}^2 = (\lambda^2 - L^2)/(1 - \kappa^2). \quad$$

Recall that we are limiting ourselves to the case $L < \lambda < D$. We finally arrive at the following expression for the free-energy functional (per unit volume) for the columnar phase:

$$f[\rho] = \frac{1}{A}\int_A d\mathbf{R}\,\rho(\mathbf{R})\left\{k_B T\{\ln[\Lambda^3\rho(\mathbf{R})] - 1\}\right.$$
$$\left. + \Delta\psi_{PHE}(\bar{\rho}(\mathbf{R})) + \frac{1}{2}h(\mathbf{R})\right\}. \quad (18)$$

By functional minimization of the free energy (18), one obtains the equilibrium density $\rho(\mathbf{R})$ at each input value of the temperature T and average number density ρ_0. For numerical convenience we assume that the columns are arranged in a two-dimensional triangular lattice with lattice parameter d (distance between neighboring columns) and express $\rho(\mathbf{R})$ as a superposition of three density waves:

$$\rho(\mathbf{R}) = \rho_0 C\exp\left(\alpha\sum_{i=1}^{3}\cos(\mathbf{k}_i \cdot \mathbf{R})\right), \quad (19)$$

where C is a constant that follows from the normalization condition $1/A\int_A d\mathbf{R}\,\rho(\mathbf{R}) = \rho_0$; $\mathbf{k}_i$ $(i = 1, 2, 3)$ are the reciprocal-lattice unit cell vectors $\mathbf{k}_1 = k(1, 1/\sqrt{3})$, $\mathbf{k}_2 = k(-1, 1/\sqrt{3})$, $\mathbf{k}_3 = k(0, 2/\sqrt{3})$, with $k = 2\pi/d$; and α in Eq.

(19) is a measure of the inverse width of the density peaks and is used here as the columnar order parameter. A value $\alpha = 0$ corresponds to the uniform nematic phase, whereas values $\alpha \neq 0$ correspond to the (hexagonal) columnar phase.

When $\rho(\mathbf{R})$ from Eq. (19) is inserted into Eq. (18), the free energy per unit volume becomes a function of the columnar order parameter α and the lattice parameter d—i.e., $f = f(T, \rho_0; \alpha, d)$. It is straightforward to obtain the explicit expression for $\bar{\rho}(\mathbf{R})$ and $h(\mathbf{R})$ in terms of α and d:

$$\bar{\rho}(\mathbf{R}) = \bar{\rho}_0(\mathbf{R}) + \bar{\rho}_1(\mathbf{R})\bar{\rho}(\mathbf{R}) + \bar{\rho}_2(\mathbf{R})\bar{\rho}^2(\mathbf{R}), \quad (20)$$

where

$$\bar{\rho}_i(\mathbf{R}) = \kappa^i\rho_0 C\int_0^{\infty} dR'\,R'\bar{w}_i(R')\int_0^{2\pi}d\phi'$$
$$\times\exp\left(\alpha\sum_{i=1}^{3}\cos[\mathbf{k}_i \cdot (\mathbf{R} + \mathbf{R}')]\right), \quad (21)$$

with

$$\bar{w}_i(R) = \int_{-\infty}^{\infty}dz\,w_i(\sqrt{R^2 + z^2}), \quad (22)$$

(R', ϕ') are the polar coordinates of vector $\mathbf{R}'$, and

$$h(\mathbf{R}) = \rho_0 C\int_0^{\infty}dR'\,R'\bar{u}_{att}(R')\int_0^{2\pi}d\phi'$$
$$\times\exp\left(\alpha\sum_{i=1}^{3}\cos[\mathbf{k}_i \cdot (\mathbf{R} + \mathbf{R}')]\right). \quad (23)$$

Within the SDA scheme, Eq. (20) reduces to a much simpler form $\bar{\rho}(\mathbf{R}) = \bar{\rho}_0(\mathbf{R})$ if one recalls that $w_1 = w_2 = 0$ under this approximation.

At given values of the average density ρ_0 and temperature T, the equilibrium properties are obtained by minimizing f with respect to the columnar order parameter α and the lattice parameter d using Powell's method [65]. Solutions with $\alpha = 0$ correspond to the nematic phase, and those with $\alpha \neq 0$ and $d \neq 0$ correspond to the columnar phase. Once the free energy is obtained from the minimization procedure, the chemical potential μ and the pressure P follow from the thermodynamic relations $\mu = (\partial f/\partial\rho_0)_T$ and $P = -f + \rho_0\mu$. Finally, the densities of the nematic and columnar phases at coexistence can be obtained at each temperature by solving the coexistence conditions of equality of the pressure and chemical potential in both phases.

IV. RESULTS

Before minimizing the free energy and solving the coexistence conditions for given sets of the potential parameters λ and L/D, we decided to check whether the nematic phase becomes unstable relative to a two-dimensional density wave modulation at fluid densities. This was accomplished by performing a bifurcation analysis [66]. We consider a density modulation in the x-y plane of the form
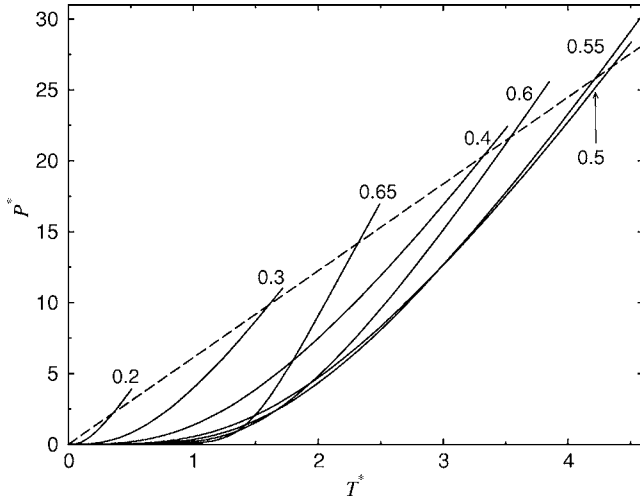
FIG. 2. Bifurcation curves showing the limit of stability of the nematic phase with respect to a density modulation in the *x-y* plane (perpendicular to the nematic director) for a system of parallel oblate hard ellipsoids with aspect ratio $L/D=0.1$ and different values of the range λ/D of the attractive well in the pressure-temperature plane. The columnar phase corresponds in each case to the low-temperature region. The dashed line represents the fluid-solid boundary line for the case $\lambda=L$ (hard spheres). The pressure and the temperature are given in reduced units $P^*=Pv_0/\epsilon$, and $T^*=k_BT/\epsilon$.

$$\rho = \rho(\mathbf{R}) = \rho_0[1 + \xi \cos(qR \cos \phi)], \qquad (24)$$

where q is the magnitude of the wave vector of the modulation along an arbitrary direction $\mathbf{q}$ (here, taken parallel to the x axis), ϕ is the angle between $\mathbf{q}$ and the two-dimensional vector $\mathbf{R}$, and ξ is a small (bifurcation) parameter ($\xi=0$ in the nematic phase). Expanding the free energy per unit volume around $\xi=0$ up to second order in ξ gives

$$f(T,\rho_0;q,\xi) = f_0(T,\rho_0) + f_2(T,\rho_0;q)\xi^2, \qquad (25)$$

where f_0 is the free energy of the nematic phase as given in Eq. (11), and

$$f_2 = \frac{1}{2}\left(\frac{\partial^2 f}{\partial \xi^2}\right)_{\xi=0}. \qquad (26)$$

Note that the linear term in Eq. (25) is identically zero due to the stability conditions. For a given temperature, the density at the bifurcation point ρ^* is the density at which the nematic phase becomes unstable with respect to a density modulation of the type given in Eq. (24). The line of bifurcation points follows from the conditions [66]

$$f_2(T,\rho^*;q^*) = 0, \quad \frac{\partial f_2}{\partial q}(T,\rho^*;q^*) = 0, \qquad (27)$$

where q^* is the magnitude of the wave vector at the bifurcation point. As a check of consistency, we first verified that in the absence of attractive interactions, our model does not stabilize columnar ordering at fluid densities.

We show in Fig. 2 the limits of stability of the nematic phase against a columnarlike density modulation in the pressure-temperature plane for a system of oblate ellipsoidal molecules with aspect ratio $L/D=0.1$ and different values of

the range of the attractive interactions $L<\lambda<D$ as obtained within the WDA. For each value of λ, the columnar phase extends over the low-temperature side of the corresponding curve in Fig. 2. As the nematic-columnar transition is first order, the bifurcation lines do not exactly correspond to the transition lines. The latter are obtained by solving the coexistence conditions of equality of the pressure and chemical potential in both phases. Our density functional theory does not incorporate the description of the solid phase, so that the stability of the columnar phase relative to a crystalline structure could not be proven. A useful guide, however, is provided by the limiting case $\lambda=L$ in which there are no attractive interactions and the system maps onto a system of hard spheres. According to Hoover and Ree [67], the fluid-solid (F-S) transition in a system of hard spheres takes place at a pressure $(Pv_0)_{FS}=6.12 \ k_BT$ and packing fractions $\eta_F=0.494$ and $\eta_S=0.545$. The corresponding fluid-solid transition line has been included in Fig. 2. For the generalized square-well model, the explicit consideration of the attractive interactions is expected to shift the melting line to lower pressures and densities. Although the extent of this shift is unkown, we can safely state that the melting line for hard spheres provides an upper limit for the stability of the fluid phase relative to the solid in the generalized square-well model.

For the smallest value $\lambda/D=0.2$, (cf. Fig. 2) it is seen that the columnar phase becomes stable relative to the nematic phase at low temperatures. At these temperatures, however, the density of the columnar phase was found to be very high. It seems plausible that full crystallization preempts the formation of the columnar phase in this case. When the square well range is increased, the theory predicts that the columnar phase becomes stable over a progresively larger region. As was found for the generalized square-well model for prolate molecules, we observe that this trend does not hold for arbitrarily large λ, but is reversed for values of λ/D larger than ≈ 0.50. Ultimately, the bifurcation equations were found to have no physical solution for values $\lambda/D \gtrsim 0.84$. According to this, the columnar phase is unstable relative to the nematic phase if the attractive interactions are too long ranged.

A further conclusion that can be drawn from Fig. 2 is that the columnar phase is not stable at arbitrarily high temperatures (or pressures) for any value of the range of the attractive interactions; it must be bounded by a nematic-columnar-solid triple point. Above this triple point, the solid would melt directly into the nematic phase. This is as expected if we bear in mind that in the high-temperature regime the attractive interactions become progressively less important (relative to the repulsive interactions) and the generalized square-well model must eventually exhibit the behavior expected for a system of hard spheres. The intersection of the nematic-columnar bifurcation line with the melting line for hard spheres provides an upper limit for the location of this triple point for each value of λ.

Several series of simulations were performed for the generalized square-well model in order to test some of the theoretical predictions. Constant *NPT* Monte Carlo simulations have been carried out. A total of $N=1600$ oblate molecules with aspect ratio $L/D=0.1$ were considered, and the range of the square well was fixed at a value $\lambda/D=0.5$. For this model parameters, our density functional theory predicts a first-

order nematic-columnar transition and a bounded region of columnar stability. The simulations were carried out in a cuboidal box with usual periodic boundary conditions applied to the x, y, and z directions. For the homogeneous nematic phase, the pressure was kept constant by performing isotropic volume fluctuations of the box. Two such trial moves were performed per cycle. When simulating the crystal or columnar phases, our constant-pressure algorithm was modified in order to allow for independent fluctuations of the box sides L_x, L_y, and L_z, but keeping the simulation box orthorhombic. When simulating phases with positional order, performing anisotropic volume fluctuations is crucial in order to avoid any unbalanced strain on the system. An attempt to change independently each of the box sides (chosen at random) was attempted per cycle. In all cases, each cycle consisted in N additional attempts to displace the particles. For a typical simulation run, we allowed the system to equilibrate for 2×10^5 Monte Carlo cycles and averages were collected for about 10^5 additional cycles. Close to a phase transition, the corresponding order parameter was seen to be subject to sluggish fluctuations. The length of the simulations in these cases was extended further until equilibrium was safely reached.

Two series of simulations were performed for each temperature. The first (expansion) series was started from a body-centered orthorhombic lattice with lattice vectors $\mathbf{a}=(a,0,0)$, $\mathbf{b}=(0,b,0)$, and $\mathbf{c}=(0,0,c)$. The axial vectors of the molecules were all pointing along the z axis and remained parallel to each other in the course of the simulations. This configuration was well equilibrated (about 5×10^5 cycles) at sufficiently high pressure. The equilibrated crystalline configuration was then slowly expanded at constant temperature in small steps in pressure. The second (compression) series was started from the same initial crystalline structure, but equilibrated at low pressure. The positional order in three dimensions is rapidly lost, and the system turns nematic. This nematic configuration was well equilibrated (5×10^5 cycles) and then slowly compressed by increasing the input pressure in small steps. Hereafter, the temperature and pressure are expressed in conventional reduced units, $T^*=k_B T/\epsilon$ and $P^*=P v_0/\epsilon$, where v_0 is the molecular volume.

The reduced pressure P^* versus packing fraction η as obtained from constant-pressure Monte Carlo simulations along three different isotherms ($T^*=1.5$, 1, and 0.75) is shown in Fig. 3. For each temperature we have included in the figure data from both the expansion and compression series of simulations. The expansion series along $T^*=1.5$ was started from a body-centered orthorhombic lattice equilibrated at $P^*=18$. The equilibrium values of the lattice parameters at this pressure were $a/D=1.0573 \pm 0.0013$, $b/D=1.4966 \pm 0.0029$, and $c/D=0.1056 \pm 0.0002$ and the average packing fraction $\eta=0.6266 \pm 0.0014$. A different crystalline structure, consisting of a closed-packed AAA stacked hexagonal lattice, was also attempted. When equilibrated at $T^*=1.5$ and $P^*=18$ this packing was seen to be unstable and rapidly evolved to a body-centered orthorhombic structure. No other crystalline structures were attempted. We also note that a body-centered orthorhombic crystal has been reported by Caprion *et al.* [41] in their simulations of the solid phase of discotic Gay-Berne molecules.
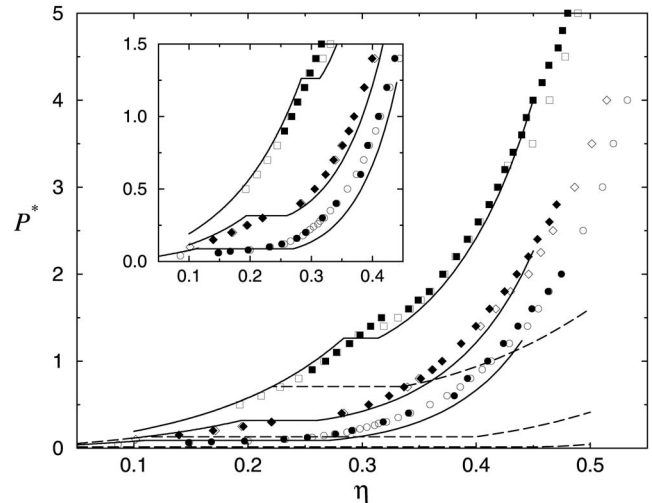

FIG. 3. Equation of state of the generalized square-well model for oblate molecules with aspect ratio $L/D=0.1$ and square-well range $\lambda/D=0.5$ along several isotherms showing nematic, columnar, and crystalline phases. From top to bottom, the temperatures are $T^*=1.5$ (squares), 1 (diamonds), and 0.75 (circles). Open symbols correspond to Monte Carlo results obtained upon expansion of a crystalline structure, and solid symbols are Monte Carlo results obtained compressing a nematic fluid. The curves are the theoretical predictions from the weighted-density approximation (solid lines) and from the smoothed-density approximation (dashed lines). The inset shows the nematic-columnar transition on a magnified scale. The pressure and temperature are given in reduced units $P^*=P v_0/\epsilon$, and $T^*=k_B T/\epsilon$; η is the packing fraction.

As seen in Fig. 3, the expansion of the orthorhombic crystal phase at $T^*=1.5$ is accompanied by a first-order transition at a pressure $P^*=3.35 \pm 0.15$ with an associated small but distinguishable discontinuity in the density. It will be shown below that the solid melts at this pressure into an hexagonal columnar phase. Upon further expansion of the system, a second transition is seen to take place at $P^*=1.35 \pm 0.05$, again accompanied by a distinct jump in the density. At this pressure the columnar phase gives way to a nematic liquid. The same sequence of phase transitions was seen along the expansion series for the other temperatures considered, the only difference being that the values of the transition pressures are correspondingly lower for decreasing temperature. We have also included in Fig. 3 the simulation data obtained by compressing the nematic liquid. At all the temperatures considered here, the nematic liquid phase was seen to undergo a first-order transition to a hexagonal columnar system at slightly higher pressures than those observed in the expansion series. Increasing the pressure of the columnar phase at constant temperature eventually gave way to the partially crystallized solid phase. As might have been anticipated, the transformation of the columnar phase into a perfect crystalline structure did not proceed along a reversible path and showed significant hysteresis.

We also include in Fig. 3 the equations of state for the nematic and columnar phases predicted by our density functional theory at the temperatures considered here. The corresponding properties at nematic-columnar coexistence have been collected in Table I and compared with our simulation

TABLE I. Values of the reduced pressure $P^* = Pv_0/\epsilon$ and packing fractions $\eta = \rho_0 v_0$ at the nematic-columnar (N-Col) transition for several values of the reduced temperature $T^* = k_B T/\epsilon$ for a system of parallel oblate molecules with aspect ratio $L/D = 0.1$ and range of the attractive interactions $\lambda = 0.5D$. Simulation data are estimates based on the *NPT* Monte Carlo expansion series (see text for details). Theoretical values are predictions from density functional theory within the weighted-density approximation (WDA) and the smoothed-density approximation (SDA).

	Simulation			WDA			SDA		
T^*	P^*	η_N	η_{Col}	P^*	η_N	η_{Col}	P^*	η_N	η_{Col}
3.0	8.55(5)	0.414(3)	0.430(5)	7.309	0.393	0.412	3.501	0.308	0.366
1.5	1.35(15)	0.301(3)	0.313(3)	1.263	0.284	0.314	0.706	0.221	0.335
1.0	0.35(5)	0.245(4)	0.273(4)	0.316	0.193	0.260	0.128	0.108	0.399
0.75	0.06(3)	0.15(3)	0.23(3)	0.088	0.111	0.271	0.013	0.018	0.454

estimates. The overall agreement between simulation and the WDA is quite satisfactory. As shown in Fig. 3, the predicted branch of the columnar equation of state falls slightly below the simulation data, the difference becoming increasingly important with decreasing temperature. The equations of state calculated within the SDA have also been included in Fig. 3. For all the temperatures considered here, the SDA is seen to predict a nematic-columnar transition but grossly underestimates the transition pressure. In addition, the density discontinuity at the transition is found to be too large when compared with the simulation data.

The nature of the different phases was assessed by monitoring the average value of appropriate order parameters during the simulations. Translational order along the z axis was probed by calculating the ensemble average of the magnitude of the leading Fourier component of the particle density along z [68]:

$$\tau(q) = \frac{1}{N}\left|\sum_{j=1}^{N}\exp(iqz_j)\right|, \qquad (28)$$

where $q = 2\pi/d_z$ is the wave vector associated with the density wave along the z axis, d_z is the corresponding wavelength, and z_j is the z coordinate of the center of mass of particle j. The above expression was evaluated for a discrete set of values of q, and the translational order parameter along $z(\tau)$ was identified with the first maximum in the values of $\tau(q)$.

Hexagonal order in the x-y plane was probed during the simulations through the calculation of the ensemble average of the (hexagonal) bond orientational order $\psi_6 = (1/N)\Sigma_i\psi_6(\mathbf{r}_i)$, where $\psi_6(\mathbf{r}_i) = \Sigma_j W(r_{ij})\exp(i6\theta_{ij})$ is the local in-plane bond order around a molecule at position $\mathbf{r}_i$. Here, θ_{ij} is the angle between the x-y projection of the intermolecular vector $\mathbf{r}_{ij}$ and an arbitrary fixed direction. The weight function $W(r_{ij})$ is defined such that only nearest neighbors contribute to the local bond order. The crystal phase is characterized by $\tau \neq 0$ (in addition, $\psi_6 \neq 0$ if the projection of the crystalline layers onto the x-y plane have hexagonal or nearly hexagonal symmetry); for the hexagonal columnar phase we expect $\tau = 0$, $\psi_6 \neq 0$; and for the nematic phase $\tau = 0$, $\psi_6 = 0$.

We show in Figs. 4 and 5 the variation of the translational order parameters τ and ψ_6 upon expansion of the crystalline

structure along three different isotherms. According to Fig. 4 the system maintains the translational order along the z axis for all packing fractions $\eta > 0.45$; in addition, ψ_6 was seen to take on values larger than 0.62 in this region, so that the system remains crystalline over this range of densities with a nearly hexagonal arrangement of the molecular centers of mass in the x-y plane. Below $\eta = 0.45$, the translational order along z is lost ($\tau \approx 0$), but the hexagonal order in the x-y plane is preserved (see Fig. 5). Therefore, the crystal melts into a hexagonal columnar phase. According to the data included in Fig. 3, the transition is first order. Interestingly, no density jump has been observed at the crystal-columnar phase transition in previous simulations of disklike molecules [29,30]. As mentioned before, a further first-order transition is observed in our simulations at lower pressures. From Fig. 5 we infer that this transition involves melting of the columnar phase into a nematic liquid at packing fractions that are temperature dependent. The density range over which columnar ordering is observed broadens with decreasing temperature. No smectic-A phase ($\tau \neq 0$, $\psi_6 = 0$) was observed at any of the temperatures investigated here. This be-
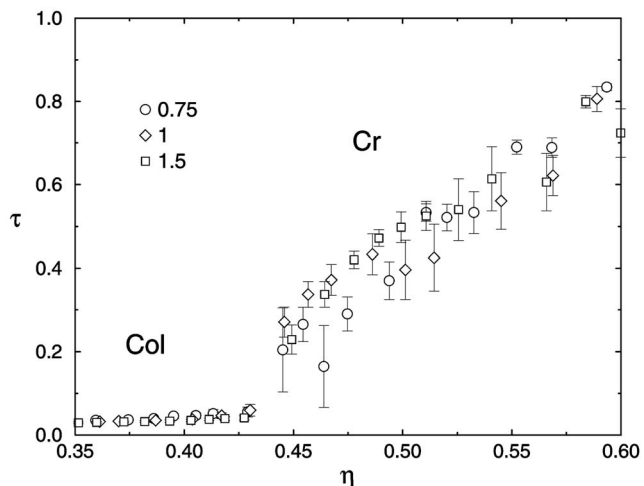

FIG. 4. Translational order parameter τ along the z axis for a system of oblate molecules interacting via the generalized square-well model with parameters $L/D = 0.1$ and $\lambda/D = 0.5$ in the neighborhood of the solid-to-columnar transition. Data are obtained from Monte Carlo expansion series at different reduced temperatures T^* labeled on the plot.
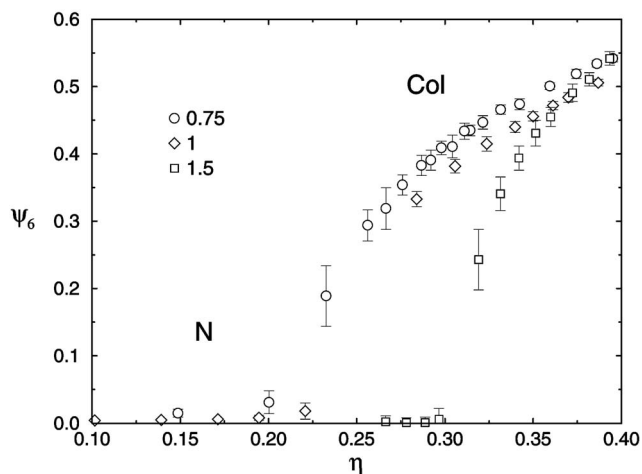
FIG. 5. Hexagonal order parameter ψ_6 in the x-y plane for a system of oblate molecules interacting via the generalized square-well model with parameters $L/D=0.1$ and $\lambda/D=0.5$ in the neighborhood of the columnar-to-nematic transition. Data are obtained from Monte Carlo simulations at different reduced temperatures T^* labeled on the plot.

havior contrasts with that of parallel cut spheres for which computer simulation shows that the smectic-A (rather than columnar) phase becomes stable between the solid and nematic phases [31].

Additional information on the structural differences of the various phases was obtained through the computation of the pair distributions $g_z(z)$ and $g_{xy}(R)$. The columnar distribution function $g_z(z)$, with $z=|z_i-z_j|$, provides information of positional correlations along the director between molecular pairs i-j within the same column. In practice, molecules i and j were considered to belong to the same column if $R=[(x_i-x_j)^2+(y_i-y_j)^2]^{1/2}$ was less than a cutoff value of $0.6D$. On the other hand, the perpendicular distribution function $g_{xy}(R)$ probes the correlations of molecular pairs in a plane perpendicular to the director. These distributions are presented in Fig. 6 for representative state points along the isotherm $T^*=1.5$. At high pressure ($P^*=18$), $g_z(z)$ exhibits a strong oscillatory behavior with nearly constant peak intensities at long distance characteristic of the solid phase. On the other hand, $g_z(z)$ is found essentially structureless at low pressure ($P^*=1$), with translational correlations that are rapidly lost beyond $z/D\approx0.5$. At a value of the pressure $P^*=2.6$, $g_z(z)$ shows an intermediate behavior, where the peak intensities are seen to decrease with increasing separation z. The absence of long-range positional correlations within the columns and the slow decay of these correlations are a clear signature of the one-dimensional liquidlike structure within the columns. The perpendicular pair distribution function $g_{xy}(R)$ is strongly peaked in the crystal phase. In addition to the peak centered at $R=0$ (due to those molecules along the **c** direction of the lattice), a number of additional peaks appear at distances R/D compatible with the expected distances in a body-centered orthorhombic structure. In the columnar phase $g_{xy}(R)$ exhibits three broad peaks at distances $R/D=d,d\sqrt{3},2d$ corresponding to the hexagonal packing of the columns, where d is the distance between neighboring columns.

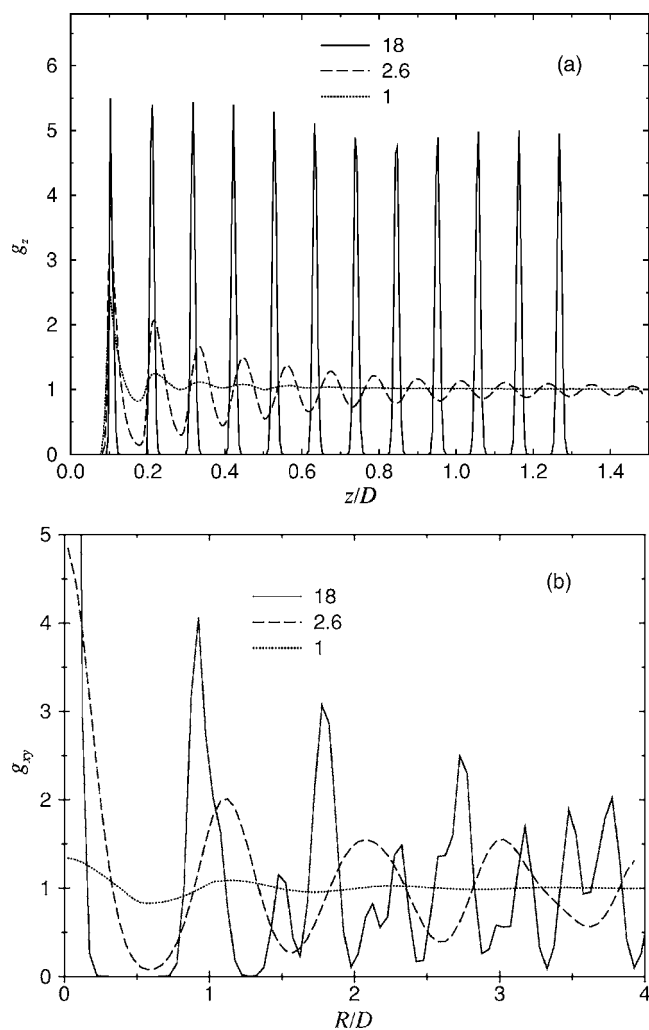
FIG. 6. (a) Columnar distribution function g_z of molecular pairs along the director (z axis) as a function of the scaled separation z/D parallel to the director and (b) perpendicular distribution function g_{xy} of molecular pairs as a function of the scaled separation R/D in the x-y plane. The distribution functions are obtained from simulation at $T^*=1.5$ and at reduced pressures of 18 (orthorhombic crystal), 2.6 (columnar phase), and 1 (nematic phase).

The hexagonal arrangement of the columns in the columnar phase is clearly illustrated in Fig. 7, where we show the x-y projection of the molecular centers of mass corresponding to the final configuration obtained at the thermodynamic conditions $T^*=1.5$ and $P^*=2.6$. The distance between neighboring columns at these conditions was found to be $d/D=1.125\pm0.005$. This value is to be compared with the value $d/D=1.158$ predicted by the WDA at this state point. The variation of the density $\rho(x,y)$ at a fixed value of y (shown in Fig. 7 by the horizontal line) is presented in Fig. 8 at a representative columnar state point ($T^*=1.5$, $P^*=2.6$). For comparison, we have included in Fig. 8 the prediction of the WDA at these conditions. The agreement can be considered quite remarkable.

As noted before, the region of stability of the columnar phase must be bounded by a nematic-columnar-solid triple point. An upper limit for this triple point is provided by the intersection of the nematic-columnar bifurcation line and the
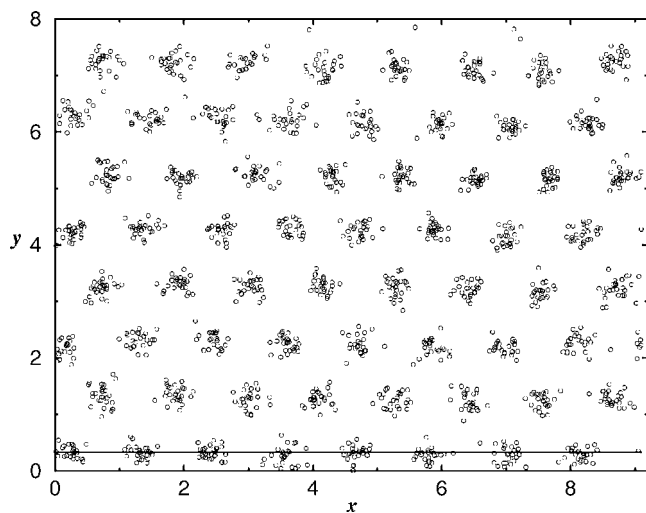
FIG. 7. Snapshot showing the projection of the molecular centers of mass onto the x-y plane of a system of $N=1600$ disklike molecules with $L/D=0.1$ interacting via the generalized square-well model with attractive range $\lambda/D=0.5$ as obtained from constant-pressure MC simulation at $T^*=1.5$ and $P^*=2.6$. At these conditions, the system exhibits columnar ordering with a hexagonal arrangement of the columns.

melting boundary line for hard spheres. According to Fig. 2, both lines cross at a value of the reduced temperature $T^*=4.27$ for $L/D=0.1$ and $\lambda/D=0.5$. Several exploratory simulation runs were performed expanding a crystal structure along different constant-temperature paths at high temperatures to test this prediction. We show in Fig. 9 the variation of the order parameters τ and ψ_6 with packing fraction at temperatures $T^*=3$ and 3.5. At $T^*=3$ the crystal phase melts into a columnar phase at $P^*=9.5$ and the latter into the nematic phase at $P^*=8.55\pm0.05$. As shown in Fig. 9, columnar ordering at $T^*=3$ is seen over a narrow range of densities when the crystal is expanded. As no free-energy calculations
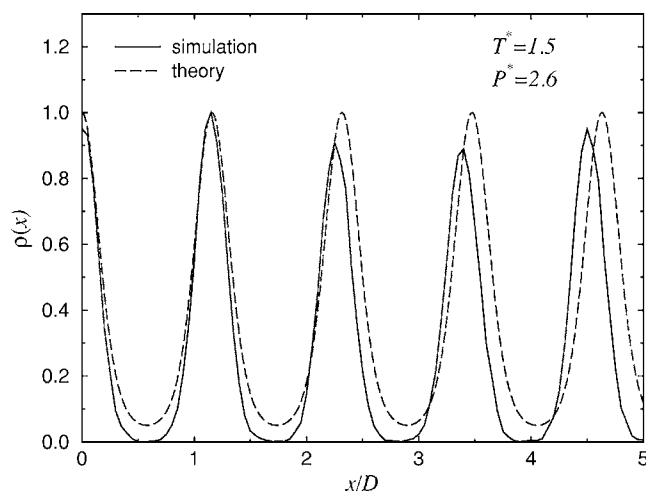

FIG. 8. Density profile $\rho(x)=\rho(x,y_0)$ in the hexagonal columnar phase ($T^*=1.5$, $P^*=2.6$) for a fixed value $y=y_0$ (indicated in Fig. 7 by the horizontal line). The solid curve corresponds to the profile obtained from simulation and the long-dashed line to the profile predicted by the WDA.
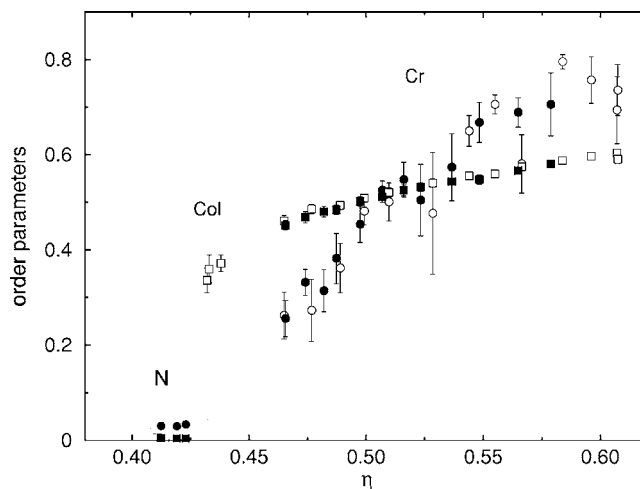

FIG. 9. Simulation data for the order parameters τ (circles) and ψ_6 (squares) as a function of packing fraction η at high reduced temperatures. At $T^*=3.5$ (solid symbols), the crystal phase (Cr) melts into a nematic (N) liquid. At $T^*=3$ (open symbols), there is a columnar phase between the crystalline and nematic phases.

have been performed in this work, it is difficult to assess the stability of the columnar phase at this temperature. At higher temperature $T^*=3.5$, both τ and ψ_6 vanished simultaneously at $P^*=11.25\pm0.25$. At this temperature, the solid phase melts directly into a nematic fluid with no intermediate columnar phase.

We summarize our results of the generalized square-well model with parameters $L/D=0.1$, $\lambda/D=0.5$ in Fig. 10 where the phase diagram of the model is depicted in the temperature-density and pressure-temperature planes. The theoretical predictions are restricted to the phase boundaries
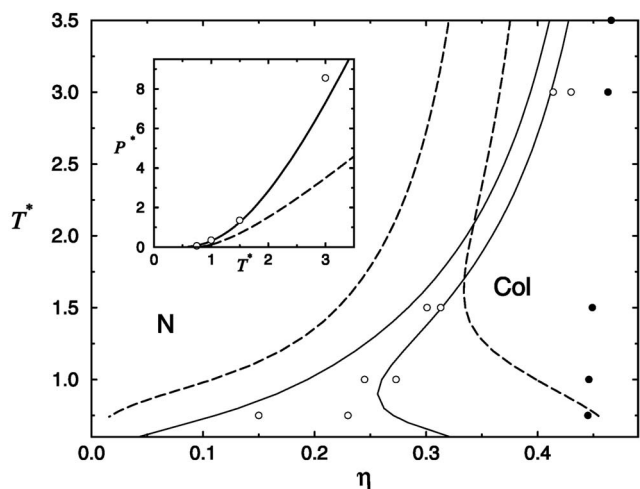

FIG. 10. Phase diagram in the temperature-density plane for the generalized square-well model with parameters $L/D=0.1$ and $\lambda/D=0.5$ as obtained from density functional theory: solid lines, WDA; dashed lines, SDA. The open symbols are estimates of the nematic-columnar transition densities from simulation (expansion runs), and the solid symbols indicate the limit of mechanical stability of the crystal phase upon expansion. The inset shows the phase diagram in the pressure-temperature plane.

of the nematic-columnar transition (recall that the description of the solid is not included in our theoretical approach). The nematic-columnar transition is predicted to be first order with a nearly constant density discontinuity at the transition except at low temperatures, where the biphasic region broadens significantly. Coexistence between two nematic phases with different densities is also predicted by the theory at low temperatures below a critical temperature $T_c^*=0.341$. However, the corresponding boundary lines lie inside the biphasic nematic-columnar region. Nematic-nematic coexistence is therefore metastable for this choice of parameters. Estimates of the coexisting densities from simulations (expansion series) have been included in the figure.

V. CONCLUSION

We have considered a simple molecular model appropriate to thermotropic discotic liquid crystals. The model is a generalization of the square-well model of simple fluids but including a nonspherical hard core. Here, we have considered the case in which the hard core has ellipsoidal symmetry and studied the stability of the columnar phase for systems of (oblate) parallel molecules. The system has been investigated in the light of a density functional theory within the weighted-density approximation, which is appropriate for strongly inhomogeneous fluid phases. When the attractive interactions are switched off, the model maps onto the hard-sphere model and no columnar phase is expected. From our theoretical analysis, this seems also to be the case when the range λ of the attractive well is small. In such cases, columnar ordering is promoted but at densities where the solid is more likely to be thermodynamically stable. This could not be definitely proven, as our formalism does not describe the solid phase. Nonetheless, our theoretical approach shows that increasing the range of the attractive interactions leads to a columnar phase at typically fluid densities. Increasing the range of the attractions increases the region over which the columnar phase is stable relative to the nematic phase. This trend, however, reverses at some intermediate value of λ, and eventually columnar ordering becomes unstable at all temperatures. These findings lead us to conclude that attractive interactions are needed in the present model to stabilize the columnar phase, but they should not be too long ranged. A further conclusion is that the columnar region is bounded at high temperature by a nematic-columnar-solid triple point.

Some of the above predictions have been tested by comparison with simulations for a given set of model parameters. For molecules with aspect ratio $L/D=0.1$ and range of the attractive well $\lambda/D=0.5$, our simulation data along a number of isotherms confirm the existence of a columnar phase between the solid and nematic phases. The free energy of the different phases was not computed, but the espontaneous formation of the columnar phase over a wide range of densities both expanding a high-density crystal and compressing a low-density nematic fluid confirms the stability of columnar ordering. As predicted by our theoretical calculations, we have also confirmed that the columnar phase is not stable at high temperatures. No smectic-A phase is observed in our simulations.

The simulation data show that the crystal-columnar and columnar-nematic transitions are first order. The theoretical predictions for the coexistence pressures and densities at the nematic-columnar transition are in fairly good agreement with the simulation estimates. It is to be remarked that a closer quantitative agreement with simulation results is only found when the weighted-density approximation is used: the nematic-columnar transition is predicted to be too strongly first order when using the smoothed-density approximation.

It would be of interest to investigate to what extent the phase behavior of the generalized square-well model is modified when orientational fluctuations are allowed for. We are currently considering a generalization of the density functional theory to systems of freely rotating molecules. Simulations of this more general case are also under way, and we hope to present the results of this investigation in the near future.

[1] S. Chandrasekhar, *Liquid crystals*, 2nd ed. (Cambridge University Press, Cambdrige, England, 1992).

[2] P. M. Chaikin and T. C. Lubensky, *Principles of Condensed Matter Physics* (Cambridge University Press, Cambdrige, England, 1997).

[3] S. Singh, Phys. Rep. **324**, 107 (2000).

[4] S. Chandrasekhar, B. K. Sadashiva, and K. Suresh, Pramana **9**, 471 (1977).

[5] N. H. Tinh, C. Destrade, and H. Gasparaux, Phys. Lett. **72A**, 251 (1979).

[6] S. Chandrasekhar, Philos. Trans. R. Soc. London, Ser. A **309**, 93 (1983).

[7] A. B. D. Brown, S. M. Clarke, and A. R. Rennie, Langmuir **14**, 3129 (1998).

[8] A. B. D. Brown, C. Ferrero, T. Narayanan, and A. R. Rennie, Eur. Phys. J. B **11**, 481 (1999).

[9] F. M. Van der Kooij and H. N. W. Lekkerkerker, J. Phys. Chem. B **102**, 7829 (1998).

[10] F. M. Van der Kooij, K. Kassapidou, and H. N. W. Lekkerkerker, Nature (London) **406**, 868 (2000).

[11] R. J. Bushby and O. R. Lozman, Curr. Opin. Colloid Interface Sci. **7**, 343 (2002).

[12] F. Pignon, J. M. Piau, and A. Magnin, Phys. Rev. Lett. **76**, 4857 (1996).

[13] M. Dijkstra, J. P. Hansen, and P. A. Madden, Phys. Rev. E **55**, 3044 (1997).

[14] E. Trizac, L. Bocquet, R. Agra, J. J. Weis, and M. Aubouy, J. Phys.: Condens. Matter **14**, 9339 (2002).

[15] T. G. Mason, Phys. Rev. E **66**, 060402(R) (2002).

[16] R. W. Samsel and A. S. Perelson, Biophys. J. **37**, 493 (1982).

[17] A. S. Perelson and F. W. Wiegel, Biophys. J. **37**, 515 (1982).

[18] L. Onsager, Ann. N.Y. Acad. Sci. **51**, 627 (1949).

[19] D. Frenkel and R. Eppenga, Phys. Rev. Lett. **49**, 1089 (1982).

[20] R. Eppenga and D. Frenkel, Mol. Phys. **52**, 1303 (1984).

[21] D. Frenkel, B. M. Mulder, and J. P. McTague, Phys. Rev. Lett. **52**, 287 (1984).

[22] D. Frenkel and B. M. Mulder, Mol. Phys. **55**, 1171 (1985).

[23] A. Stroobants, H. N. W. Lekkerkerker, and D. Frenkel, Phys. Rev. Lett. **57**, 1452 (1986).

[24] A. Stroobants, H. N. W. Lekkerkerker, and D. Frenkel, Phys. Rev. A **36**, 2929 (1987).

[25] D. Frenkel, Mol. Phys. **60**, 1 (1987).

[26] J. L. Lebowitz and J. W. Perram, Mol. Phys. **56**, 4213 (1983).

[27] M. A. Bates and D. Frenkel, Phys. Rev. E **57**, 4824 (1998).

[28] M. A. Bates and D. Frenkel, J. Chem. Phys. **110**, 6553 (1999).

[29] J. A. C. Veerman and D. Frenkel, Phys. Rev. A **45**, 5632 (1992).

[30] S.-D. Zhang, P. A. Reynolds, and J. S. van Duijneveldt, J. Chem. Phys. **117**, 9947 (2002).

[31] H. Azzouz, J. M. Caillol, D. Levesque, and J. J. Weis, J. Chem. Phys. **96**, 4551 (1992).

[32] J. G. Gay and B. J. Berne, J. Chem. Phys. **74**, 3316 (1981).

[33] E. de Miguel, L. F. Rull, M. K. Chalam, and K. E. Gubbins, Mol. Phys. **74**, 405 (1991).

[34] J. T. Brown, M. P. Allen, E. Martín del Río, and E. de Miguel, Phys. Rev. E **57**, 6685 (1998).

[35] M. A. Bates and G. R. Luckhurst, J. Chem. Phys. **110**, 7087 (1999).

[36] E. de Miguel and C. Vega, J. Chem. Phys. **117**, 6613 (2002).

[37] E. de Miguel, E. Martín del Río, and F. J. Blas, J. Chem. Phys. **121**, 11183 (2004).

[38] A. P. J. Emerson, G. R. Luckhurst, and S. G. Whatling, Mol. Phys. **82**, 113 (1994).

[39] M. A. Bates and G. R. Luckhurst, J. Chem. Phys. **104**, 6696 (1996).

[40] H. Zewdie, Phys. Rev. E **57**, 1793 (1998).

[41] D. Caprion, L. Bellier-Castella, and J. P. Ryckaert, Phys. Rev. E **67**, 041703 (2003).

[42] K. K. Kobayashi, J. Phys. Soc. Jpn. **29**, 101 (1970).

[43] W. L. McMillan, Phys. Rev. A **6**, 936 (1972).

[44] P. Tarazona, Philos. Trans. R. Soc. London, Ser. A **344**, 307 (1993).

[45] A. M. Somoza and P. Tarazona, Phys. Rev. A **40**, 4161 (1989).

[46] R. Holyst and A. Poniewierski, Mol. Phys. **71**, 561 (1990).

[47] R. P. Sear and G. Jackson, J. Chem. Phys. **102**, 2622 (1995).

[48] T. Coussaert and M. Baus, J. Chem. Phys. **116**, 7744 (2002).

[49] H. H. Wensink, Phys. Rev. Lett. **93**, 157801 (2004).

[50] N. Boden, R. J. Bushby, G. Cooke, O. R. Lozman, and Z. B. Lu, J. Am. Chem. Soc. **123**, 7915 (2001).

[51] E. O. Arikainen, N. Boden, R. J. Bushby, O. R. Lozman, J. G. Vinter, and A. Wood, Angew. Chem., Int. Ed. **39**, 2333 (2000).

[52] F. M. van der Kooij, M. Vogel, and H. N. W. Lekkerkerker, Phys. Rev. E **62**, 5397 (2000).

[53] W. M. Gelbart and B. A. Baron, J. Chem. Phys. **66**, 207 (1977).

[54] E. Martín del Río and E. de Miguel, Phys. Rev. E **71**, 051710 (2005).

[55] P. Tarazona, Phys. Rev. A **31**, 2672 (1985).

[56] D. R. Evans, G. T. Evans, and D. K. Hoffman, J. Chem. Phys. **93**, 8816 (1991).

[57] B. Tjipto-Margo and G. T. Evans, Mol. Phys. **74**, 85 (1991).

[58] E. de Miguel and M. P. Allen, Mol. Phys. **76**, 1275 (1992).

[59] S. Varga and I. Szalai, Mol. Phys. **95**, 515 (1998).

[60] S. Varga, D. C. Williamson, and I. Szalai, Mol. Phys. **96**, 1695 (1999).

[61] E. García, D. C. Williamson, and A. Martínez-Richa, Mol. Phys. **98**, 179 (2000).

[62] P. Tarazona, Mol. Phys. **52**, 81 (1984).

[63] L. Mederos and D. E. Sullivan, Phys. Rev. A **39**, 854 (1989).

[64] P. Tarazona, U. M. B. Marconi, and R. Evans, Mol. Phys. **60**, 573 (1987).

[65] W. H. Press, S. A. Teukolsky, W. T. Vetterling, and B. P. Flannery, *Numerical Recipes* (Cambridge University Press, Cambridge, England, 1986).

[66] B. Mulder, Phys. Rev. A **35**, 3095 (1987).

[67] W. G. Hoover and F. H. Ree, J. Chem. Phys. **49**, 3609 (1987).

[68] J. M. Polson and D. Frenkel, Phys. Rev. E **56**, R6260 (1997).